

PROCEEDINGS OF SPIE

SPIEDigitalLibrary.org/conference-proceedings-of-spie

Suitability of explosive simulants for millimeter-wave imaging detection systems

James C. Weatherall, Duane Karns, Jeffrey Barber, Barry T. Smith, Peter R. Smith

James C. Weatherall, Duane Karns, Jeffrey Barber, Barry T. Smith, Peter R. Smith, "Suitability of explosive simulants for millimeter-wave imaging detection systems," Proc. SPIE 10994, Passive and Active Millimeter-Wave Imaging XXII, 109940G (13 May 2019); doi: 10.1117/12.2521723

SPIE.

Event: SPIE Defense + Commercial Sensing, 2019, Baltimore, Maryland, United States

Suitability of Explosive Simulants for Millimeter-Wave Imaging Detection Systems

James C. Weatherall^a, Duane Karns^a, Jeffrey Barber^b, Barry T. Smith^b, and Peter R. Smith^c

^aBattelle Memorial Institute, 2900 Fire Road, Suite 201, Egg Harbor Township, NJ 08234 USA

^bU.S. Department of Homeland Security, Science and Technology Directorate, Transportation Security Laboratory, William J. Hughes Technical Center, Atlantic City NJ 08405 USA

^cAASKI Technology, Inc., 1 Radar Way, Tinton Falls, NJ 07724 USA

ABSTRACT

The test and evaluation of millimeter-wave imaging systems for explosive detection is facilitated by the substitution of explosive simulants which have an identical response to millimeter-wave illumination. The primary detection feature for millimeter-wave imaging is the dielectric constant (or electrical permittivity), so the approach to developing simulants is to match the complex dielectric constants of explosives to inert simulant materials at frequencies relevant to the imaging system. This paper describes a measurement-based methodology to assure that the simulant is a suitable substitute for the explosive. The methodology is demonstrated by dielectric measurement at 86 GHz to establish a simulant for ethylene glycol dinitrate (EGDN).

Keywords: Millimeter wave, image quality, reflection coefficient, dielectric constant, permittivity, Advanced Imaging Technology, EGDN

1. INTRODUCTION

Millimeter-wave imaging systems are used at checkpoints and airports for screening of persons for explosives. The evaluation of these systems against new threats, and the development of new algorithms for automatic target recognition (ATR), requires the use of explosives as test objects. The inherent risks and limitations in using explosives, and homemade explosives (HME) and their precursors, makes the substitution of explosive simulants with identical response to millimeter-wave illumination useful and desirable. The primary detection feature for millimeter-wave imaging is the dielectric constant (or electrical permittivity), so the approach to developing simulants is to match the complex dielectric constants of explosives to inert simulant materials at frequencies relevant to the imaging system.¹

This begs the question of how well the simulant will perform as a substitute for the explosive: in particular, if the imaging characteristics of the explosive are indistinguishable from the simulant. We describe here a laboratory measurement-based approach to quantifying the differences in the response of the two materials to millimeter-waves, and a test to establish to a particular statistical significance that the differences are, or are not, detectable.

This proceedings paper presents the major concepts in the simulant vs. explosive comparison. In Sec. 2, the factors for MMW anomaly detection in imaging systems are described; issues relating to collection of experimental data are discussed in Sec. 3; the elements to demonstrating simulant suitability based on statistical testing are formulated in Sec. 4, and a trial case is presented in Sec. 5. Section 6 is a summary.

2. FACTORS IN MMW ANOMALY DETECTION

In Advanced Imaging Technology (AIT) based on millimeter-wave imaging, the detection of image anomalies derives from reflectivity, or image intensity. A list of imaging attributes affecting the reflectivity, and the underlying physical features, is given in Table 1.

Further author information: (Send correspondence to J.C.W)
Email: james.weatherall@associates.hq.dhs.gov

Table 1. Factors in MMW Anomaly Detection

Image attribute	Physical feature
Front surface reflection	Dielectric constant Package layering Frequency
Absorption (penetration)	Dielectric loss Geometry (thickness) Frequency
Internal reflection	Dielectric constant Geometry (thickness) Backing layer Frequency Frequency bandwidth
Diffraction (edges)	Dielectric constant Geometry (size, shape) Phase (solid, liquid, powder) Frequency
Scattering	Dielectric constant Texture (surface) Homogeneity (volume) Frequency

2.1 Permittivity as Primary Detection Feature

Of the physical features in the Table 1 (excluding for the moment the macroscopic aspects relating to surface texture and homogeneity), the only feature intrinsic to the material is the dielectric constant, or permittivity. Consequently, for millimeter wave imaging, the electrical permittivity is identified as the primary physical quantity correlating to detection, and can be used for the comparison of simulant to explosive. This means that permittivity, measured on laboratory instruments, can be used to compare the imaging attributes detected by commercial millimeter-wave imaging systems. This conclusion is supported by Maxwell's equations, which describe in total the effects of materials on electromagnetic wave propagation processes – including reflection, refraction, scattering, and diffraction – in terms of the electrical permittivity and magnetic permeability. Because explosives are generally nonmagnetic, the role of magnetic permeability is less relevant and is not treated further here. More discussion of how the permittivity relates to millimeter-wave imaging can be found in Ref. 2.

2.2 External Features

Other image attributes are either system-dependent, such as the imaging frequency and frequency bandwidth, or depend on factors under external control, such as the geometry, layering, packaging, and what is behind the sample. However, it can be anticipated that given a match in permittivity between explosive and simulant, the materials will be optically equivalent if they are configured in exactly the same way. The equivalence is further facilitated when explosives and simulants that are powders or liquids have similar forms in order to match flow properties when packaged in bags, for example. Similarly, for multi-component explosives, reflection fidelity to effects of scattering can be obtained by matching dielectric constant and size of the individual components. Surface texture can also be reproduced when scattering is an important imaging attribute.

The system-dependent features are also important. Because the dielectric constant is rooted in the atomic and molecular dynamics of materials, it is frequency dependent.³ The dielectric constant can be significantly different across frequencies for which the material's polarization response changes – the effect of dielectric relaxation.

Because the dielectric “constant” is not constant, it is important that the measurements supporting the use of a simulant be made at the frequency associated with the imaging system.

3. INSTRUMENTATION

Frequency is one of the considerations for dielectric measurement, but the choice of instrumentation is also affected by whether the material has high or low dielectric constant, and whether it is transparent or opaque to millimeter-waves.

Consider that millimeter-wave imaging characteristics of explosives and simulants are sensitive to absorption in the material; this is because transparent or semi-transparent materials have reflections from multiple surfaces. Absorption is associated with the imaginary component of the dielectric constant and must be accurately measured. Commercial dielectric measurement apparatus such as dielectric probes measure the imaginary component to a precision of 5% of the dielectric constant magnitude;⁴ thus, for low dielectric materials, such as $|\epsilon| \sim 2.5$, the probes cannot accurately measure materials for $\text{Im } \epsilon < 0.1$, which is still moderately absorptive. Alternatively, resonant cavity measurement systems^{5–7} are capable of measuring $\text{Im } \epsilon$ to as low as 0.001. Probes can be useful at high dielectric and high loss, but they are generally limited to less than 50 GHz by the operating range of the measurement network analyzer. Because of the variability of frequency, dielectric constant, and absorptive properties, required instrumentation for documenting dielectric constants may range from resonant cavities, dielectric probes, and free space systems.⁸

4. DIELECTRIC EQUIVALENCE REQUIREMENTS

To apply comparison based on experimental measurement, the first step is to specify the match in reflection coefficient that qualifies the equivalency between the simulant and explosive. Then, the dielectric matching requirement (i.e., the dielectric bounding box) will be the range in dielectric values that will achieve the reflection criterion. The latter requires an analytic model to incorporate a range of external and system features that factor into the image.

4.1 Reflectivity Resolution

One way to specify the reflection equivalence is based on the intensity resolution of the system. Consider that the detected reflectivity in an imaging system has variation due to system noise and the image reconstruction process. For example, in Barber, et al.,¹ the grayscale distribution of a flat metal target for an imaged phantom had a standard deviation of approximately 4 – 5%, i.e. $\sigma_r/r \sim 0.05$. Thus, differences on this order are unlikely to be resolved. A graphical representation of two such *unresolved* grayscale distributions is shown in Fig. 1.

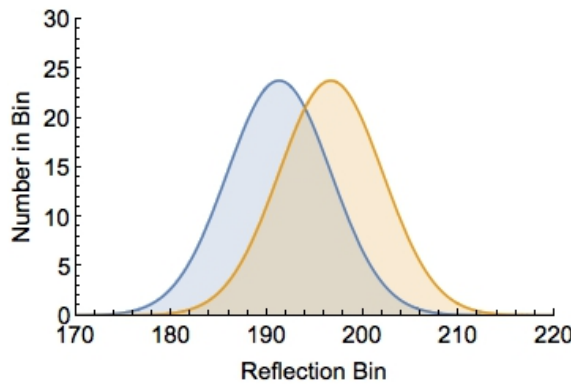


Figure 1. Two normal distributions of reflection coefficient whose means are separated by one-half of one standard deviation. The data from 324 pixels are binned in 8-bit data.

The smallest detectable difference in two overlapping distributions has an analog in spectroscopy known as the Houston criterion,^{9,10} which recognizes that two distributions are distinct when their means differ by 2.355σ .

The Houston criterion applies to distributions that cross at half-max points. The criterion can be viewed as a *sufficient* condition for two reflection coefficients to be distinguishable, but may or may not be the same as the *necessary* condition to cause a difference in detection. In the following, we adopt the Houston criterion as the reflection requirement.

4.2 Relating Dielectric to Reflection Coefficient

The net reflection coefficient is connected to the complex permittivity through Fresnel equations for layered materials.^{11,12} The total of the reflected electric field has contributions from reflections on the front and back surface, and multiple internal reflections that escape the slab. Scaled to the incident wave electric field, the reflected field is a function of frequency, ω , and can be written as a sum:

$$E(\omega) = r_1 + t_0 r_2 t_1 (e^{i\theta_1} + (r'_1 r_2) e^{i\theta_2} + (r'_1 r_2)^2 e^{i\theta_3} + \dots). \quad (1)$$

The r and t terms are the Fresnel reflection and transmission coefficients for fields at a single layer-interface.¹³ In terms of the material layer's refractive index, n , the reflection and transmission coefficients propagating from air into the material are $r_1 = (n-1)/(n+1)$ and $t_1 = 2n/(n+1)$; and the reflection and transmission coefficients for fields propagating outward from the material into air are $r'_1 = (1-n)/(1+n)$ and $t_0 = 2/(1+n)$. The reflection coefficient at the back interface is $r_2 = (n_2 - n)/(n_2 + n)$, where n_2 is the index of refraction of the back material. The index of refraction is a function of the permittivity, $n = \sqrt{\epsilon}$. The net reflection coefficient is a function of frequency because the reflections from the front surface and back surface (and other internal reflections) interfere constructively or destructively, depending on frequency. The phasing for m-propagations to-and-from the front and back surface separated by a thickness L depends on the frequency according to

$$\theta_m = m \frac{n \omega}{c} 2L. \quad (2)$$

In holographic imaging systems, the reflection image is an amalgam of frequencies, where the frequency data is incorporated into the image reconstruction algorithm to map in three-dimensions. Therefore, in image processing, the phases in Eq. (1) can become uncorrelated because the phasing in the imaging does not take into account the frequency-dependent delay in the layer due to the refractive index not being unity. The phases will become mismatched in phase by more than one radian (57 degrees) when the thickness L is greater than the coherence length, $\hat{L} \sim (c/\Delta\omega)(n-1)^{-1}$. The coherence length in millimeter-wave imaging systems is typically 1 cm or less. The loss of phase coherence in the image reflectivity can be modeled with an ensemble average over a Gaussian function with bandwidth $\Delta\omega$ and central frequency $\omega_0 = 2\pi f_0$:

$$\langle r^2 \rangle = \frac{1}{2\pi\Delta\omega} \int_0^\infty \exp\left[-\frac{(\omega - \omega_0)^2}{2\Delta\omega^2}\right] |E(\omega)|^2 d\omega \quad (3)$$

Equations (1) - (3) incorporate the material-specific dielectric properties, the system-dependent factors, and the external factors, all into the reflection coefficient.

4.3 Dielectric Bounding Box

The dielectric bounding box is the range of dielectric values that produce the same reflection coefficient as the dielectric constant of the explosive, within the accuracy of the reflection equivalence criterion. The dielectric bounding box is determined by computing the reflection coefficient through the reflectivity model (Eq. 1) for a dielectric space in the vicinity of the targeted dielectric constant for the explosive, $\epsilon_e = \epsilon'_e + i\epsilon''_e$. For this calculation, the system-dependent and external factors are required. The system-dependent factors are defined by the system intended for use of the simulant; the external factors (i.e., the dielectric target thickness, L , and refractive index of the material behind the dielectric target, n_2), are specified case-by-case for anticipated imaging scenarios. The test value ϵ will be in the bounding box if for the test case,

$$\left| r(\epsilon' + i\epsilon'') - r(\epsilon'_e + i\epsilon''_e) \right| \leq 2.355 \sigma_r. \quad (4)$$

Recall that the factor 2.355 derives from the resolution criterion. Testing a large number of dielectric values defines the limits of the bounding box. The bounding box may include multiple cases by simulating a range of anticipated thicknesses and backing materials. The bounding box will be illustrated with the example in Sec. 5.

4.4 Comparison Methodology

The comparison of permittivity of the two materials is based on measurement and associated uncertainties. The comparison is made using mean values for the real and imaginary dielectric components of the explosive and simulant. The confidence interval for the comparison also depends on the number of independent measurements, the desired statistical significance, and the multiplicity of statistical tests.

For example, the confidence limits for the measure of difference in the two population means for real dielectric component would be given by

$$\bar{\epsilon}'_s - \bar{\epsilon}'_e \pm t_c \sqrt{\frac{\sigma'_s{}^2}{N_s} + \frac{\sigma'_e{}^2}{N_e}} \quad (5)$$

Here, σ'_e (σ'_s) and N_e (N_s) are the standard deviations and number of measurements in ϵ'_e (ϵ'_s). t_c is the critical value for the confidence level, which is set at $\alpha = 0.05$, or 95%. Probability theory calculates the critical value $t_{.95}$ from a Student's distribution with $(N_e - 1) + (N_s - 1)$ degrees of freedom.

4.5 Equivalence Test

The equivalence testing is performed with the “two-one-sided t-test” (TOST) procedure.^{14,15} The procedure is done separately for the real and imaginary component of the dielectric constant. In TOST, two composite null hypotheses are tested: one is that the dielectric constant constant difference is less than the lower bounding box limit; and, second, that the dielectric constant difference is greater than the upper bounding box limit. The null hypothesis will be rejected if it fails either t-test at the $\alpha = 0.025$. Here, the α -value for the cumulative distribution function is reduced by a factor of 1/2 as a Bonferroni correction because two statistical tests are required from the data (one for the real component, and another for the imaginary component). With rejection of the null hypothesis, the alternate hypothesis is established that the two means are equivalent at the specified confidence level.

The equivalence established by the TOST procedure is operationally identical to showing that the confidence interval for $\bar{\epsilon}_e - \bar{\epsilon}_s$ with $\alpha = 2 \times 0.025$ is contained within the bounding box limits.¹⁴ The confidence interval approach is an expedient way to demonstrate the equivalence test.

Finally, in order to guard against the test falsely accepting equivalence, the statistical power of the test can be evaluated *a posteriori* from analytical formulary.¹⁶ The statistical probability should have $\beta = 0.2$ or less, or a statistical power of at least 80%.

5. ACCURACY OF A LIQUID EXPLOSIVE SIMULANT

A liquid simulant for EGDN explosive was assessed as an example of the methodology described above. The results are presented in this section.

The system-dependent factors correspond to a broadband of sub-cm wavelengths. For this evaluation, we require an accuracy of 8% in the reflectivity ($\sigma_r = 0.08$). For external factors, we include a range of thickness and background reflectivity. The permittivity measurements are given in Table 2. A resonant cavity⁵ was used for the measurements, at the nominal resonant frequency of 86 GHz. Eleven samples of the explosive were measured, and ten samples of the simulant material were measured.

The bounding box – the dielectric region which produces an equivalent reflectivity to the explosive – is computed according to the procedure in Sec. 4.3. The bounding box is plotted in the complex dielectric plane in Fig. 2, with the explosive at the origin.

Table 2. Dielectric Data

Material	$\epsilon' \pm \sigma'$	$\epsilon'' \pm \sigma''$
Explosive	4.46 ± 0.11	1.12 ± 0.14
Simulant	4.29 ± 0.20	1.17 ± 0.14

The differences in the real and imaginary components of the dielectric constants of the explosive and simulant are summarized in Table 3, together with the respective confidence interval for the 95% significance test. The critical value for $\alpha = 0.05$ is $t_c = 3.1$.

Table 3. Difference in Dielectric Constant Measurements

Dielectric Mismatch	Confidence Interval		
$\bar{\epsilon}'_s - \bar{\epsilon}'_e$	-0.17	$t_c \sqrt{\frac{\sigma'^2_s}{N_s} + \frac{\sigma'^2_e}{N_e}}$	0.12
$\bar{\epsilon}''_s - \bar{\epsilon}''_e$	0.05	$t_c \sqrt{\frac{\sigma''^2_s}{N_s} + \frac{\sigma''^2_e}{N_e}}$	0.07

The confidence interval for the dielectric difference between simulant and the explosive is plotted in Fig. 2. Because the confidence interval is entirely within the bounding box region, the statistical hypothesis of equivalence is established at the 95% significance level. The power of the test is greater than 80%, as required.

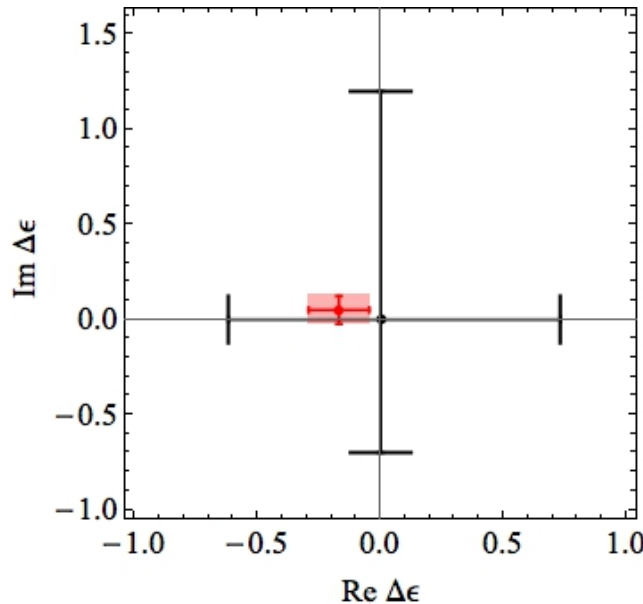


Figure 2. Confidence interval (CI) and bounding box limits for equivalence test of explosive and simulant in dielectric space centered at $\epsilon_e = 4.46 + 1.12i$. The difference in dielectric constant $\epsilon_s - \epsilon_e$ is indicated with error bars for the CI, and is shaded for emphasis. The bounding limits for equivalence are indicated with hatch marks.

6. CONCLUSION

A method to establish the equivalence of a millimeter-wave simulant to an explosive using laboratory measurements was described. The procedure involves comparing the permittivity of the two materials. Other factors considered are set by system-dependent features, such as operating frequency range and sensitivity, and external variables, such as thickness and reflection from the back surfaces. The functional equivalence is established by a test of specified statistical significance and power. The procedure was demonstrated by assessing a simulant for a liquid explosive using dielectric measurements of both materials.

ACKNOWLEDGMENTS

The simulant and surrogate validation program is funded by DHS S&T contract HSHQDC-13-A-00023 under contract task HSHQDC-16-J-00448. Research and development in millimeter-wave technology is supported by task HSHQDC-15-J-00395 DHS S&T, and DHS Contract No. 70RSAT18D00000003, task 70RSAT18FR0000162. The development of high fidelity simulants development is performed under contract task 70RSAT18FR0000174. Dr. Joseph Palma (Battelle) has guided much of the simulant verification work, in coordination with scientific staff at the Transportation Security Laboratory of the DHS/S&T.

REFERENCES

- [1] Barber, J., Weatherall, J. C., Smith, B. T., Duffy, S., Goettler, S. J., and Krauss, R. A., "Millimeter wave measurements of explosives and simulants," in [*Passive Millimeter-Wave Imaging Technology XIII*], *SPIE Proceedings* **7670**, 76700E (2010).
- [2] Barber, J., Weatherall, J. C., Brauer, C. S., and Smith, B. T., "Development of a contrast phantom for active millimeter-wave imaging systems," in [*Sensors, and Command, Control, Communications, and Intelligence (C3I) Technologies for Homeland Security and Homeland Defense X*], *SPIE Proceedings* **8019**, 80190G (2011).
- [3] Keysight Technologies, "Keysight N1501A Dielectric Probe Kit 10 MHz to 50 GHz." Technical Overview No. 5992-0264 [Online] <https://www.literature.cdn.keysight.com/litweb/pdf/5992-0264EN.pdf> (2018). (Accessed: June 2018).
- [4] Keysight Technologies, " Basics of Measuring the Dielectric Properties of Materials." Application Note, literature number 5989-5384 [Online] <http://literature.cdn.keysight.com/litweb/pdf/5989-2589EN.pdf> (2019). (Accessed: February 2019).
- [5] Karns, D. C., Weatherall, J. C., Greca, J., Smith, P. R., Yam, K., Barber, J., and Smith, B. T., "Millimeter-wave resonant cavity for complex permittivity measurements of materials," in [*2018 IEEE/MTT-S International Microwave Symposium-IMS*], 1006–1009 (2018).
- [6] Weatherall, J. C., Barber, J., Smith, P. R., Smith, B. T., and Greca, J., "Electromagnetic modeling of a millimeter-wavelength resonant cavity." 2016 COMSOL Conference, Boston [Online] https://www.comsol.dk/paper/download/361691/weatherall_paper.pdf (2016). (Accessed: June 2018).
- [7] Weatherall, J. C., Barber, J., and Smith, B. T., "Resonant system and method of determining a dielectric constant of a sample," (Dec. 12 2017). US Patent 9,841,448.
- [8] Smith, P. R., Weatherall, J. C., Barber, J., Yam, K., Greca, J., and Smith, B. T., "Measurements of the dielectric properties of explosives and inert materials at millimeter wave frequencies (V-band and above) using free space reflection methods," in [*Passive and Active Millimeter-Wave Imaging XX*], *SPIE Proceedings* **10189**, 1018908 (2017).
- [9] Jones, A., Bland-Hawthorn, J., and Shopbell, P., "Towards a general definition for spectroscopic resolution," in [*Astronomical Data Analysis Software and Systems IV*], **77**, 503 (1995).
- [10] Houston, W. V., "The fine structure and the wave-length of the balmer lines," *The Astrophysical Journal* **64**, 81 (1926).
- [11] Weatherall, J. C., Barber, J., and Smith, B. T., "Identifying explosives by dielectric properties obtained through wide-band millimeter-wave illumination," in [*Passive and Active Millimeter-Wave Imaging XVIII*], *SPIE Proceedings* **9462**, 94620F (2015).
- [12] Smith, B. T., Weatherall, J. C., and Barber, J. B., "Method for identifying materials using dielectric properties through active millimeter wave illumination," (Feb. 3 2015). US Patent 8,946,641.
- [13] Jackson, J. D., [*Classical Electrodynamics*], John Wiley & Sons (1999).
- [14] Schuirmann, D. J., "A comparison of the two one-sided tests procedure and the power approach for assessing the equivalence of average bioavailability," *Journal of pharmacokinetics and biopharmaceutics* **15**(6), 657–680 (1987).
- [15] Westlake, W., "Bioequivalence testing—a need to rethink," *Biometrics* **37**(3), 589–594 (1981).
- [16] Shieh, G., "Exact power and sample size calculations for the two one-sided tests of equivalence," *PloS one* **11**(9), e0162093 (2016).